Integration of simulation and analysis software

Abstract

Here we consider the benefits of linking various simulation methods with existing analysis codes. The project is motivated by the desire to provide users with additional tools to help them better understand their data. Examples have been selected where initial work has already been carried out and where a clear development path and user requirement exists. The list, however, is by no means exhaustive, and there will be many other simulation techniques that can make similar contributions. Some of the examples discussed herein may be selected and their application further developed as part of the work this task area.

The magnetic dipolar field is characteristic of the muons location in its host material. Codes developed during the Joint Research Activities (JRA) in NMI3-I provide a means of calculating them and we consider the benefits of integrating these with existing analysis codes. The Quantum package simulates the interactions originating from coupled spin systems. We consider how the package might be integrated with analysis codes and further developed to include data fitting functionality which would allow parameters such as dipolar, hyperfine and quadrupole couplings to be fitted and later extracted by the user. This might help, for example, identify the muon binding site or charge carrier hopping rates. *ab initio* Density Functional Theory (DFT) can be an effective method for calculating hyperfine coupling interactions, knowledge of which is essential for the interpretation of Avoided Level Crossing (ALC) experiments. This not only provides the experimenter with an indication of the appropriate field regions that need to be scanned during an experiment, but also should help assign resonances to nuclei and identify the muon binding sites during data analysis. This document also considers how instrument simulation codes might be used to help interpret the results of μSR experiments.

Contents

Jamie Peck (jamie.peck@stfc.ac.uk)

September 2013

1 Calculation of magnetic dipolar fields, nuclear or electronic in origin

Background

Knowledge of the positive muon site in a material is frequently crucial to properly understanding the muon response and for revealing the physics of the sample. Unfortunately, making an unambiguous site determination is not straightforward and a best guess is often required, frequently made by considering a combination of the structural, chemical and physical properties of the material. Significant work continues to be carried out to improve methods for determining the muon site, and for a recent comprehensive discussion see J.S. Möller *et al* [1].

Dipolar field calculations are particularly useful for gaining an insight into the muon location. Starting with knowledge of the lattice structure, nuclear dipolar fields can readily be calculated and a muon response simulated. Candidate muon localisation site(s) can be deduced through a comparison to experimental results. Work carried out during the JRA in NMI3-I developed methods for extending this procedure to samples with electronic magnetism, although in this case knowledge of the magnetic structure is important. Applications of nuclear dipolar field calculations are illustrated by the following case studies.

Case study 1: Muon sites in $Ca(OH)_2$

In this case the zero field signal (Figure 1, left) could be described by either a damped oscillation or a Gaussian decay (at short time). However, a Kubo-Toyabe was a poor model for the long time behaviour of the data. Muon depolarisation arising from nuclear dipolar couplings could be calculated for candidate muon sites in the crystal and compared to the initial Gaussian decay (0.293(3) μs^{-1}). Remarkable agreement (0.291 μs^{-1}) was obtained for a muon occupying a proton site with coupling to neighbouring protons in the material (Figure 1, right). The calculations enabled the formation of the MuOH to be ruled out as this species would have a considerable larger muon depolarisation rate (0.49 μs^{-1}). Knowledge of the muon site enabled detailed modelling using Quantum [2], that confirmed the unusual behaviour at long times was the result of a highly anisotropic non-Gaussian field distribution at the muon site. For further details see S.P. Cottrell et al. [3].

Case study 2: Muon sites in heavy Fermion materials

Obtaining information about magnetic properties and spin dynamics is the prime motivation for studying heavy fermion materials. Unfortunately crystal structures are typically complex for this class of material and, as a local probe, knowledge of the muon site in the compound is important for data interpretation. The heavy fermion compound $CeInPt_4$ (Figure 2, left) was recently studied by Hillier et al. [4]. In this case, information about nuclear couplings and the muon site was obtained by measuring in a temperature regime where the contribution to the depolarisation from electronic spin fluctuations was minimal, while the muon could be demonstrated as static in the structure. Because of the complexity of the system, software was developed to enable contour plots to be made of the muon depolarisation for selected crystallographic planes (Figure 2, right). Comparison with the experimental muon depolarisation

identified the most likely muon location within the unit cell at $(\frac{1}{2}, \frac{1}{2}, \frac{1}{4})$ and at equivalent sites.

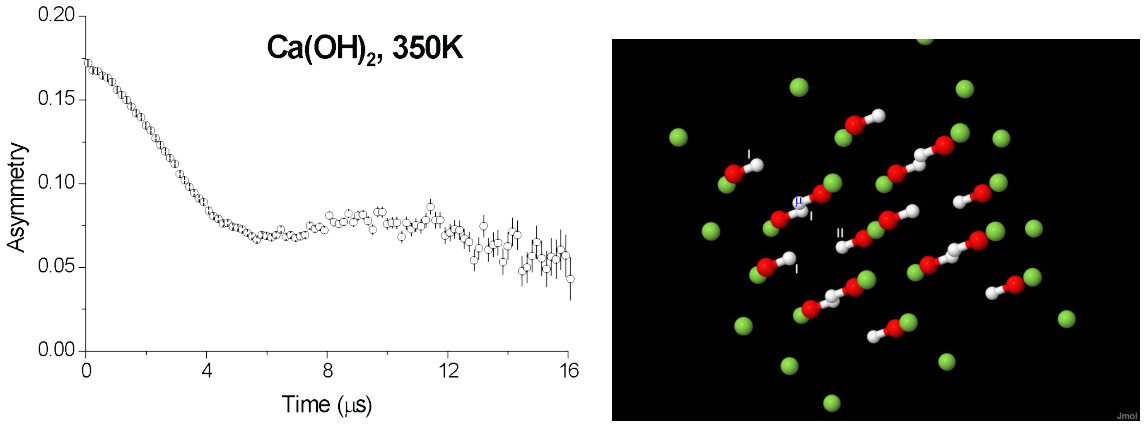

Figure 1: *Zero field measurement of $Ca(OH)_2$ (left) and crystal structure (right) with H shown in white and O in red.*

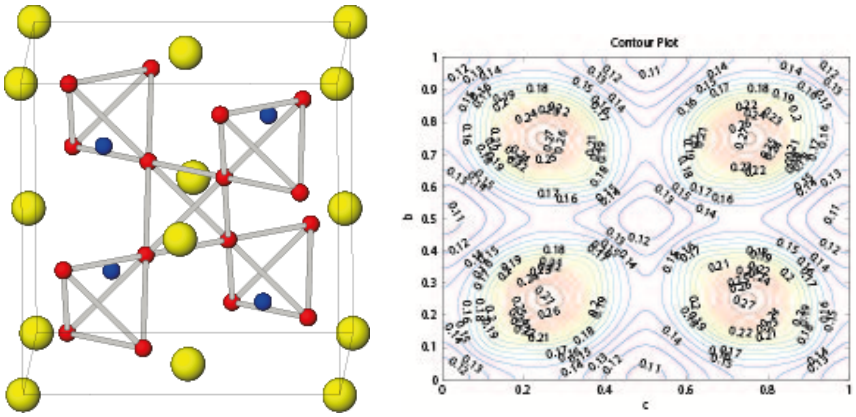

Figure 2: *Crystal structure of $CeInPt_4$ (left), with In shown in blue, and a contour plot of muon depolarisation (right).*

Summary

These studies illustrate the potential benefit of having access to dipolar field calculations during data analysis. The codes make a valuable contribution to data interpretation through an ability to select candidate muon sites. To date, however, such routines have been developed by individual groups to meet specific requirements, and have generally not been made available to the wider user community. Work within this task area will investigate how this might be addressed, perhaps by coding a stand-along package for dipolar field calculations, and consider how these codes might be included within an analysis framework such as Mantid (see reference [5]). Merging analysis and simulation codes brings an immediate advantage of giving facility users a single package for exploring their data, but may later enable the development of more complex fitting routines where simulation results are used directly by the least squares fitter.

2 Integrating Quantum with analysis codes

Background

Quantum is a program that uses the density matrix method for simulating the interaction between a series of spins, such as a muon and its neighbouring electrons and nuclei. It includes parameters such as dipolar, hyperfine and quadrupole interactions, external magnetic fields (static or RF) and fluctuations. Either single crystals with a defined orientation, or powder averages can be simulated. At present Quantum is a stand-alone program, with the ability to read and write data files in ASCII format. Quantum can plot simple line graphs of time domain data or integral scans, however, it is usually necessary to write the result to a file and re-read it into a separate data plotting package. Integration with an existing analysis code would give users a single package to explore data while providing a path to full data fitting.

Simulating effects such as ALC resonances, zero field nuclear dipolar relaxation, or relaxation rates as a function of field helps the experimenter to extract hyperfine constants, muon sites, or charge carrier hopping rates. The user can estimate these parameters from independent calculations, using them as input for the Quantum simulation and comparing the result of the simulation with real data. The parameters can then be modified based on comparison with the real data. Simulation results might be used by least squares fitting routine included in the analysis package to automatically refine simulation parameters. The following two case studies help demonstrate the capabilities of the Quantum package.

Case Study 1: Simulated LCR in muoniated benzene

Roduner et al. observed the level crossing resonances associated with the interaction of the muon, unparied electron, and spin $\frac{1}{2}$ H nuclei in the cyclohexadienyl radical [6]. Figure 3 (right) shows the experimental spectrum of the cyclohexadienyl radical recorded at 263 K where the Δ_0 resonance is associated with $A_{e\mu}$=519.7 MHz while the Δ_1 resonance was found to be associated with A_{ep}=126.5 MHz from the *ipso* proton. The quantum mechanical simulation shown in Figure 3 employed these parameters as input, along with anisotropies of $D\mu$=3.5 MHz and D_p=0.9 MHz. The simulation reproduces the resonance position, width and intensity with excellent accuracy, demonstrating the usefulness of these simulations in the analysis of ALC data. In this particular case, values for $A_{e\mu}$ and A_{ep} were determined by Transverse field experiments. However, they could also be obtained by comparing the Quantum simulation with the measured data through trail and error, or, if the software is integrated, they might be extracted from the least squares fitting routine following their refinement.

Case Study 2: Muon sites in $Ca(OH)_2$ and $Cd(OH)_2$

Dipolar field calculations allowed the muon binding sites in $Ca(OH)_2$ and $Cd(OH)_2$ to be assigned. The proposed binding site in both materials was similar and resulted in a highly anisotropic coupling. The muon is bound within the lattices in such a way that it is strongly coupled to three protons and together, form a roughly planar system. The zero-field μSR measurements of $Ca(OH)_2$ and $Cd(OH)_2$ are shown in Figure 4. Both materials exhibit an unusual behaviour at long times that cannot be described by a kubo-Toyabe model. With knowledge of the binding sites from dipolar calculations, Quantum was used to simulate the muon relaxation (shown

as solid lines in both plots), providing excellent agreement with the experimental data at short and longer times, thus providing additional confirmation of the proposed binding site. Further details can be found in reference [3].

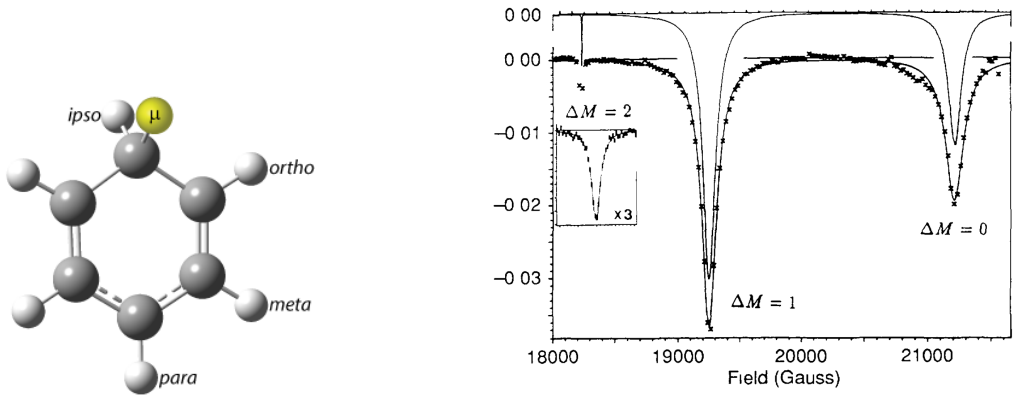

Figure 3: *Benzene muoniated radical (left). Experimental vs. simulated spectrum collected by Roduner et al. [6] (right).*

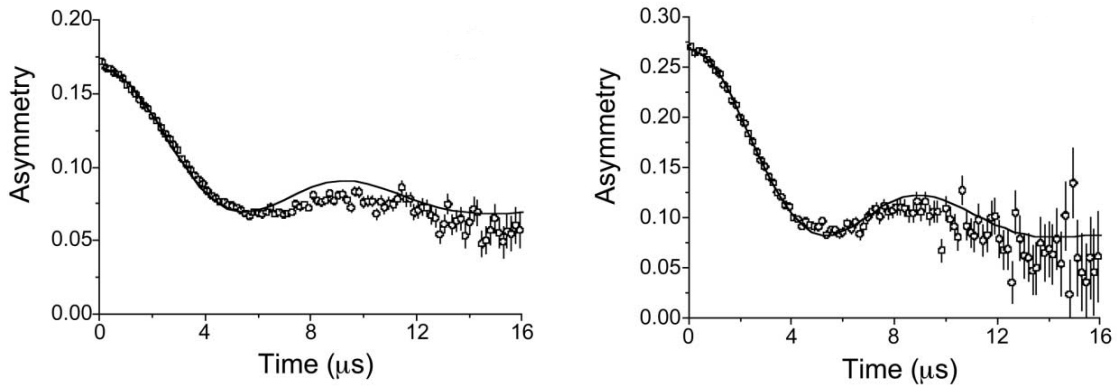

Figure 4: *Zero field measurements of $Ca(OH)_2$ (left) and $Cd(OH)_2$ (right) recorded at 350 and 403 K, respectively. The solid lines are associated with fits of the data obtained using Quantum [3].*

Summary

The additional insight that density matrix methods provide in these examples is evidence of the value it offers to μSR data interpretation. These benefits could be enhanced and made more accessible to the user community by integrating Quantum with an existing analysis code. Since ISIS has adopted Mantid [5] as its choice analysis code, work is likely to involve demonstrating this integration with the Mantid package.

The present version of Quantum is a compiled executable for Windows, though it can run in a virtual machine on other operating systems. The new version could be distributed as Python code and should therefore run on any operating system (Windows, Mac and most Linux versions). Quantum uses the density matrix formalism and therefore performs a lot of matrix manipulation. It currently does this using the IMSL library from Fortran, the new version could be coded in Python using the numpy library routines. Mantid also uses numpy arrays for much

of its internal processing. The bulk of the processing takes place in the library routines so the speed of the wrapper code is not so critical. The use of Python also allows Quantum to be more portable. For example, using C++, either directly or as a wrapper around the original Fortran code, would require that Quantum was compiled for each of the operating systems supported by the Mantid and re-linked every time a new version of the Mantid is released. While this could be simplified by including Quantum into Mantids code repository and automatic build system, it would then be much harder to add one-off modifications, as is often requested by users.

3 Calculation of hyperfine coupling interactions

Background

Calculation of muon-electron and nuclear-electron hyperfine coupling constants (HFCC's) using *ab initio* methods is used to assist the interpretation of Avoided Level Crossing (ALC) μSR experiments. Muonium (μ^+e^-) rapidly reacts with centres of unsaturation (double or triple bonds) to form a muoniated radical species. The spins of the muon, unpaired electron, and spin nuclei within the sample interact with each other though the isotropic and anisotropic components of the hyperfine interaction, A, forming a quantised system described by a series of discrete energy levels. At certain magnetic fields, the energy levels in the muon and sample system become nearly degenerate, and are able to interact through A. During this interaction the spins oscillate between the two energy states resulting in a dip in the polarisation, which is observed as a resonance as the magnetic field is incrementally scanned. The magnitude of the muon-electron, $A_{e\mu}$ and nuclear-electron, A_{ep} are characteristic of the muon binding site, and give rise to ALC resonances whose position are dependant upon their magnitude. Calculating the muon and nuclear HFCC's therefore allows estimation of the resonance positions, prior knowledge of which has the potential to save valuable time by allowing the the experimenter to scan only the necessary field regions. Additionally, the experimenter is able to assign resonances to nuclei and identify the muon binding site by comparing the measured and simulated HFCC's. However, for this to be successful, an understanding of the accuracy to which these values can be calculated is first required.

There are several software packages that facilitate calculation of hyperfine coupling interactions. Packages such as Gaussian [7] and Vienna Ab initio Simulation Package (VASP) [8] require licences, which may restrict their accessibility. However, open source packages such as GAMES, Amsterdam Density Functional (ADF) and Orca are also well maintained, but these still involve a difficult installation process and a steep learning curve in order to be able to extract meaningful results.

The input of a typical calculation requires specification of the atomic coordinates, the charge and multiplicity of the species, and definition of a model chemistry (theoretical method and basis set). With this information the structure of a molecule and its properties such as hyperfine interactions can be predicted. In order to accurately predict the magnitude of hyperfine coupling interactions it is crucial to have an accurate description of the spin density at nuclear positions. This is reliant on a suitable choice of basis set, and given that each has a limited atomic palette and suitability for particular applications, this is a difficult choice. It is therefore necessary to consult the literature to ensure the suitability of a choice. For some applications studies are low in number, so it may be necessary to construct a training set of molecules of similar composition to validate a particular theoretical method/basis set. Accounting for the effects of dynamics and solvation present additional difficulties and a review by Improta and Barone discusses suitable methods of overcoming them [9].

Case study: Comparison of experimental and simulated hyperfine interactions for the muoniated cyclohexadienyl radical.

The cyclohexadienyl muoniated radical was one of the first to be studied using the μSR technique [10], and is now considered a classic prototype system in muoniated radical chemistry [6, 11]. When muonium reacts with a unsaturated C-C bond in benzene, the cyclohexadienyl radical is formed, with the unpaired electron density delocalised throughout the ring. It is therefore possible to observe an $A_{e\mu}$ hyperfine coupling and *ipso*, *orhto*, *meta* and *para* nuclear couplings. Data reported in Table 1 compares experimental values for $A_{e\mu}$ and *ipso* A_{ep} with simulated values obtained using a selection of functionals in combination with the EPR-III basis set. Post optimisation, it was necessary to lengthen the C-Mu bond by 4.9 % and perform a single-point calculation in order to account for the larger zero-point energy of the muonium bond [12]. Additionally, in order to mimic the larger gyromagnetic ratio of the muon relative to the proton, $A_{e\mu}$ values are scaled by 3.1833. At ~263 K, the experimental Δ_1 resonance appears at a field of 1.9084 Tesla, associated with a $A_{e\mu}$ of 519.7 MHz [6]. The PBEO/EPR-III calculation gives good agreement with this, with only an 104 Gauss shift. The magnitude of the proton coupling was systematically overestimated by ~15 MHz by all functionals, again the PBEO/EPR-III level gives closest agreement. However, at this level of theory the resonance is predicted to be 874 Gauss lower than the experimental resonance position. The PBE functional overestimates both $A_{e\mu}$ and A_{ep} by 11.4 MHz and 16.9 MHz, respectively, meaning the Δ_1 is predicted to appear 301 Gauss lower than the experimental. New scaling factors could be used to improve the predictions, but these would need to be validated on a training set of molecules of similar composition.

Table 1: *Comparison of experimentally determined and simulated $A_{e\mu}$ and ipso A_{ep} hyperfine coupling constants of the cyclohexadienyl muoniated radical at 263 K. Calculations employ a variety of functionals, in all cases using the EPR-III basis set.*

	$A_{e\mu}$ (MHz)	$\Delta_1 B_{res}$ (T)	A_{ep} *ipso* (MHz)	$\Delta_0 B_{res}$ (T)
Exp.[(a)]	519.7	1.9084	126.5	2.1040
HF	525.6	1.9302	140.9	2.0580
TPSS	546.1	2.0055	146.6	2.1375
B3LYP	525.1	1.9284	141.7	2.0514
PBE	531.1	1.9502	143.4	2.0739
PBEO	516.8	1.8980	139.9	2.0166

[(a)] *Data selected from [6].*

Summary

There is a definite need to develop a better understanding of how to simulate hyperfine interactions in radical species. The example highlights the difficulties associated with these calculations. Firstly, there are issues with actually running the simulation - the user having access to the codes, and making a suitable choice of the theoretical method. Secondly, there is the problem of accuracy. Previous studies have demonstrated that no one level of theory is capable of accurately predicting hyperfine interactions in different classes of systems - basis sets have only a limited compatibility/accuracy across the elements in the periodic table [9]. Additional difficulties arise when trying to model aliphatic radical species and such cases necessitate quantum

mechanical averaging of the hyperfine interactions in order to model the real system. If the scale factors implemented for prototype systems can be applied to more complicated analogue systems, it might be possible to integrate the software codes and produce a single user interface. This would allow the user to simulate ALC resonances by first calculating $A_{e\mu}$ and A_{ep}. Work in the task could include further investigations into the benzene radical and analogue systems: accurately predicting the magnitudes of the ortho, meta, and para proton couplings, and applying this methodology to predict couplings in substituted benzene analogues.

4 Instrument simulation

Background

Understanding how the design of a muon spectrometer and its sometimes elaborate sample environments effect the behaviour of the incoming muon beam and the outgoing positrons is essential for the interpretation of experimental data. Simulations allow properties such as the instrument geometry, build materials, and field profile to be defined, and the response to muons and decay positrons modelled. While the original application of many codes focused on instrument design and development, we now explore whether it is possible for users to apply these codes to enhance the interpretation of experimental data.

Case study 1: Simulating the GPD detector

This study illustrates how investigating the muon stopping site distribution and the background in the General Purpose Decay-Channel (GPD) detector array at PSI using *musrSimAna* helped Sedlak et al. to interpret their data [13]. Simulations allowed the experimenter to characterise both the background and sample signals. Figure 5 (left) shows a cross-section of the GPD detector, indicating positron counters (blue), the M-counter (red), the collimators (green), and a high pressure sample cell containing the sample (small concentric circles). Figure 5 (centre) shows a histogram describing the distribution of all the detected muon events in this cross-section. The majority of muons stop and decay in either the sample or sample cell, but some stops occur in the M-counter, the detectors, or the collimators. All of these muon stops contribute to the overall signal. The simulation helped to identify the various contributions in the measured signal, allowing the user to develop a fitting model which accounted for the various signal components.

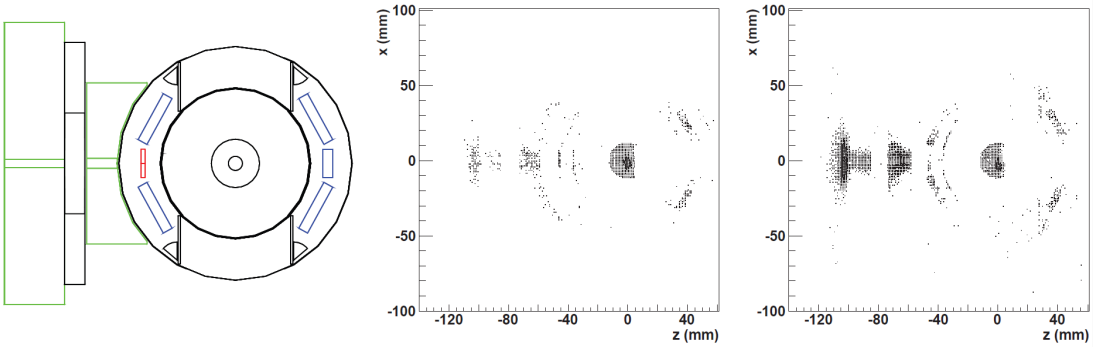

Figure 5: *musrSim simulation of the cross-section of a GPD detector (left). musrSimAna simulations of muon stopping sites for all detected events (centre) and pileup of muons μ_2 (right) [13].*

Case study 2: Simulating the field distribution in a pressure cell loaded with a sample with nonzero magnetisation

In experiments making use of so-called clamped pressure cells, typically less than one half of all the muons stop within sample, with the rest stopping in the pressure cell walls. For example, this is the case when using the GPD instrument located at PSI. Samples, placed within a pressure cell, and possessing a strong magnetisation will induce a sizeable magnetic field around

them when an external field is applied. This spatially inhomogeneous induced field leads to an additional depolarisation of the muon spin polarisation, which depends on the applied field, the sample magnetisation and the spatial distribution of the stopped muons. Simulations performed by Alexander Maisuradze were specifically made in order to account for the stray fields induced by magnetic (diamagnetic) samples placed inside a pressure cell [14]. Selected results of these simulations for a ferromagnetic sample are presented in Figure 6. Such simulations allow a better understanding of the response of the muons fraction stopped in the pressure cell walls and therefore lead to a better determination of the sample signal.

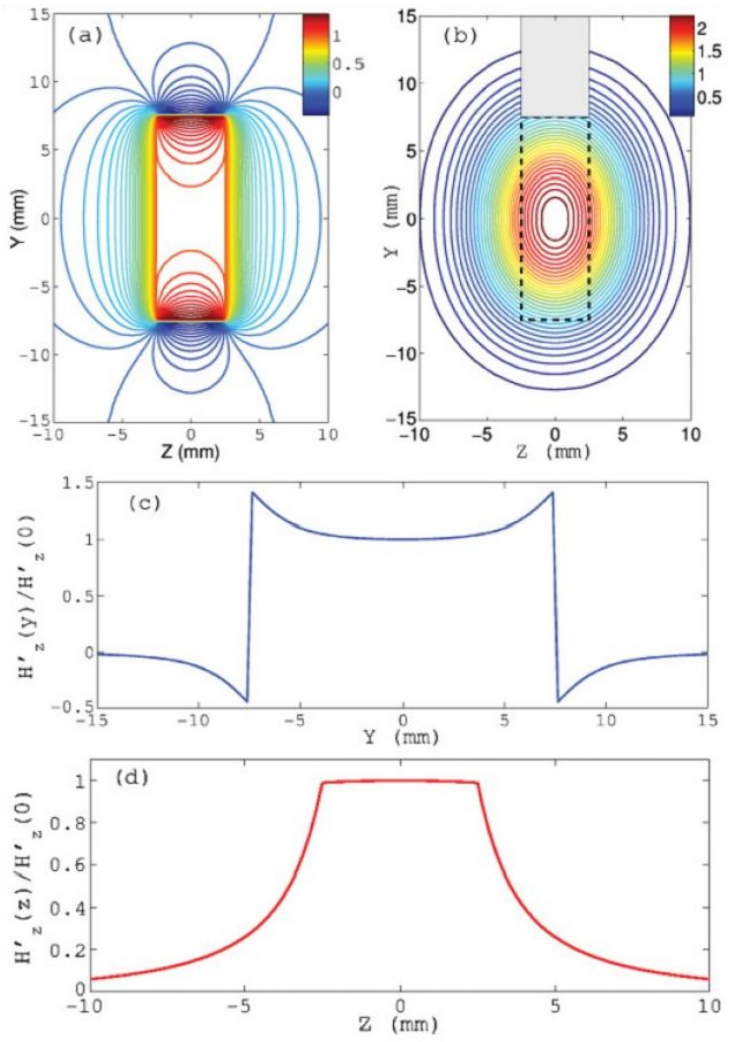

Figure 6: *(a) Contour plot of the field distribution $H(y, z)$ in the yz plane for a cylindrical sample with radius 2.5 mm and a height of 15 mm. (b) Contour plot of the muon stopping distribution in the yz plane. The dashed line indicates the sample space. (c) Magnetic field profile along the y axis and (d) magnetic field profile along the z axis.*

Case study 3: Simulating cells for laser excitation

Photomusr experiments are known for their challenging nature, not least because of the difficulty in characterising muon stopping distribution and cell background, but mainly because of the challenge of ensuring muon stops are coincident with the area irradiated by the laser. The kinetics of the Mu + H_2^*(v=1) → MuH + H reaction were investigated by Bakule et al. [15].

This required that H_2 be in its v=1 energy level, and this was achieved using stimulated Raman pumping (SRP). However, these reaction kinetics could only be accessed in the area with overlapping muon stops and laser irradiation, a small area considering an elliptical laser profile of 1x14 mm. Figure 7 (right) shows a plot of the measured Mu asymmetry (black circles and squares) and simulated asymmetry (red dashed line) as a function of degrader thickness. Excellent agreement exists between the measured data and the GEANT4 simulation, with both showing a maximum asymmetry associated with a ~600 μm degrader. The muonium asymmetry in the laser beam as a function of degrader thickness was then simulated using GEANT4 (shown as dashed black line in Figure 7) and for this case a maximum muonium asymmetry was predicted with a ~450 μm mylar window. The simulations therefore provided additional information that not only helped optimise the experimental set-up, but also later in the interpretation of the measured data.

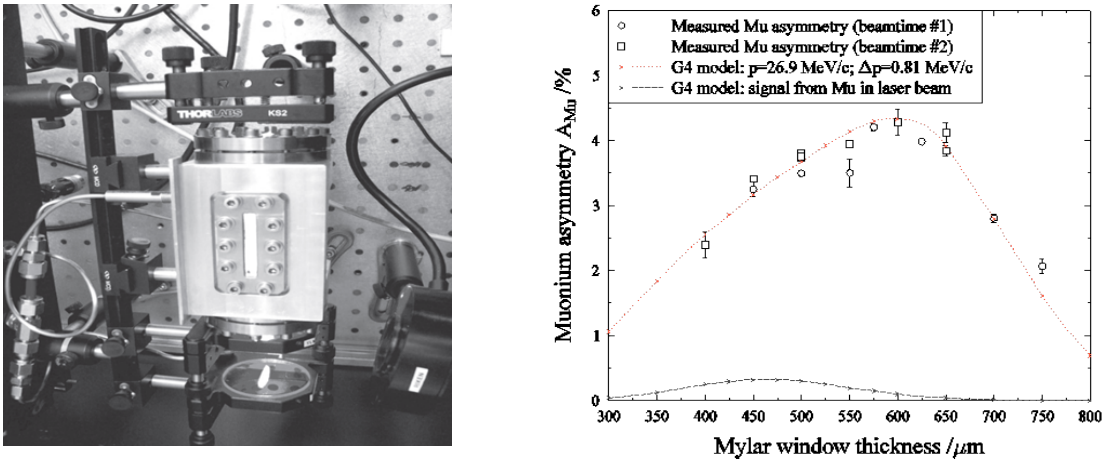

Figure 7: *Muon gas cell (left) and comparison of the measured asymmetry with simulated asymmetry from the model cell* (unpublished material)*(right).*

Summary

These examples demonstrate how codes developed for μSR instrument simulation and development, might contribute to experimental data analysis. The ability to simulate muon trajectories should enable the user to investigate the contribution of sample and background signals to the measured signal, facilitating the development of an accurate fitting model. For the laser cell, the simulation results proved key to understanding how to set-up the experiment and interpret data, suggesting these types of simulation can contribute to the complex experiments that are becoming increasingly common. This task could consider further applications for this type of simulation, for example, in characterising gas and RF cells, or samples mounted in the flypast configuration.

References

(1) J. S. Moller et al., *Playing quantum hide-and-seek with the muon: localizing muon stopping sites*, 2013, arXiv:1307.0651v1[cond-mat.str-el]2Jul2013.

(2) J. S. Lord, 'Computer simulation of muon spin evolution', *Phys. B*, 2006, **374–375**, 472–474.

(3) S. Cottrell, J. Lord and W. Williams, 'Proton sites and dynamics in divalent metal hydroxides probed by muon spin relaxation', *J. Phys. Chem. Solids*, 2001, **62**, 1977 –1983.

(4) A. D. Hillier, D. T. Adroja, S. R. Giblin, W. Kockelmann, B. D. Rainford and S. K. Malik, 'Understanding the heavy fermion behavior in $CeInPt_4$', *Phys. Rev. B*, Nov. 2007, **76**, 174439.

(5) *Mantid*, http://www.mantidproject.org.

(6) E. Roduner, 'Polarized positive Muons probing free radicals: a variant of magnetic resonance', *Chem. Soc. Rev.*, 1993, **22**, 337–346.

(7) M. J. Frisch et al., *Gaussian 03, Revision E.02*, Gaussian, Inc., Wallingford, CT, 2004.

(8) http://cms.mpi.univie.ac.at/marsweb/.

(9) R. Improta and V. Barone, 'Interplay of Electronic, Environmental, and Vibrational Effects in Determining the Hyperfine Coupling Constants of Organic Free Radicals', *Chem. Rev.*, 2004, **104**, 1231–1254.

(10) E. Roduner, G. A. Brinkman and P. W. Louwrier, 'Muonium-substituted organic free radicals in liquids. Muon-electron hyperfine coupling constants and the selectivity of formation of methyl and fluorine-substituted cyclohexadienyl type radicals', *Chem. Phys.*, 1982, **73**, 117–130.

(11) D. G. Fleming, D. J. Arseneau, M. Y. Shelley, B. Beck, H. Dilger and E. Roduner, 'μSR Studies of Hyperfine Couplings and Molecular Interactions of the Mu-Cyclohexadienyl Radical in Y-Zeolites and in Solid Bulk Benzene', *J. Phys. Chem. C*, 2011, **115**, 11177–11191.

(12) E. Roduner and I. D. Reid, 'Hyperfine and structural isotope effects in muonated cyclohexadienyl and cyclopentyl radicals', *Isr. J. Chem.*, 1989, **29**, 3.

(13) K. Sedlak, R. Scheuermann, T. Shiroka, A. Stoykov, A. Raselli and A. Amato, 'MusrSim and MusrSimAna - Simulation Tools for μSR Instruments', *Physics Procedia*, 2012, **30**, 61 –64.

(14) A. Maisuradze, A. Shengelaya, A. Amato, E. Pomjakushina and H. Keller, 'Muon spin rotation investigation of the pressure effect on the magnetic penetration depth in $YBa_2Cu_3O_x$', *Phys. Rev. B*, Nov. 2011, **84**, 184523.

(15) P. Bakule et al., 'Toward the first study of chemical reaction dynamics of Mu with vibrational-state-selected reactants in the gas phase: The reaction by stimulated Raman pumping', *Phys B*, 2009, **404**, 1013 –1016.